J. Fluid Mech. (2006), *vol.* 564, *pp.* 185–196. © 2006 Cambridge University Press
doi:10.1017/S002211200600142X Printed in the United Kingdom

Thermal vibrational convection in near-critical fluids. Part 2. Weakly non-uniform heating

By D. LYUBIMOV[1], T. LYUBIMOVA[2], A. VOROBEV[1]†, A. MOJTABI[3] AND B. ZAPPOLI[4]

[1]Theoretical Physics Department, Perm State University, Perm, 614990, Russia
[2]Institute of Continuous Media Mechanics, Perm, 614013, Russia
[3]Institut de Mecanique des Fluides, Toulouse, 31062, France
[4]Centre National d'Etudes Spatiales, Toulouse, 31055, France

(Received 23 October 2003 and in revised form 6 March 2006)

The governing equations and effective boundary conditions to describe thermal vibrational convection in a near-critical fluid are derived with the help of the multiple-scale method and averaging procedure. In contrast to Part 1, this paper focuses on the effects of density non-homogeneities caused not by external heating but by vibrational and gravity stratifications due to the divergent mechanical compressibility of near-critical media. It is shown that vibrations generate non-homogeneities in the average temperature, which result in the onset of thermal convection even under isothermal boundary conditions. An agreement with the results of previous numerical and asymptotical analyses and with experiments is found.

1. Introduction

The objective of our work is to investigate of the average effects of translational high-frequency vibrations on the behaviour of near-critical fluids. We assume that the period of oscillation of a container is much smaller than the typical convective time, i.e. $\omega \gg (\nu/L^2, \chi/L^2)$, where ν, χ are the coefficients of kinematic viscosity and thermal diffusivity, ω is the frequency of oscillation, and L is the typical size of the container. This criterion can be interpreted as small thicknesses of the boundary layers induced by vibrations, in comparison with the size of the container:

$$\delta_\nu = \sqrt{\frac{\nu}{2\omega}} \ll L, \quad \delta_\chi = \sqrt{\frac{\chi}{2\omega}} \ll L. \tag{1.1}$$

Here δ_ν, δ_χ are thicknesses of the viscous and thermal skin layers.

According to the main idea of the multiple-scales method we divide all the hydrodynamic equations into two parts, separately describing average and pulsating flows. In a similar way we derive the effective boundary conditions by examining the fluid behaviour inside the boundary layers. An example of the derivation is given in Part 1 (Lyubimov *et al.* 2006).

A near-critical fluid implies a medium in a condition close to the thermodynamic critical point (figure 1).

† Present address: The University of Michigan – Dearborn, Dearborn, MI 48128, USA.

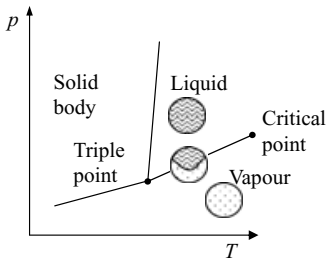

FIGURE 1. Phase diagram in the temperature–pressure plane.

A review of the model and methods we use, together with references on vibrational convection and developments in the hydrodynamics of near-critical fluids are available in Part 1. That part dealt with near-critical fluids subjected to translational vibrations in the presence of imposed external temperature differences. Vibrations were shown to induce not only pulsational flows, but also the average motion. The necessary condition to generate the average flows was the imposed temperature gradient.

Nevertheless, owing to mechanical compressibility, temperature gradients might also be generated by other factors, e.g. vibrational forcing or gravity stratification. Since the mechanical compressibility of a near-critical medium is divergent, these temperature gradients become significant.

In Part 1 we supposed that an imposed temperature difference θ was of the second order in ϵ, $\theta = O(\epsilon^2)$ (where $\epsilon = (T - T_c)/T_c$, and T_c is the critical temperature) and the above-mentioned additional temperature non-homogeneities were insignificant. However, if the imposed temperature gradient is even smaller, $\theta = o(\epsilon^2)$, or absent (isothermal boundary conditions), the temperature non-homogeneities induced by vibrations or gravity may result in additional mechanisms for the generation of average motion.

The paper is organized as follows. In § 2 we formulate the theoretical model of thermal vibrational convection for the case of weak boundary heating and, as a particular case, for isothermal boundary conditions. Using the model derived we examine the stability of a plane fluid layer and the generation of average flows in a cylindrical cavity subjected to translational vibrations. A comparison with known results is provided to validate the model. Section 3 is devoted to the situation when there is neither gravity nor external heating. Nevertheless, under intensive vibrations, average temperature variations induced at the boundary layers are able to generate average flows in the bulk. A comparison with available direct numerical simulations is also provided. In § 4 we formulate the conditions for the selection of a particular model of thermal vibrational convection (among those obtained in Parts 1 and here). The main conclusions of the work are summarized in § 5.

2. Weakly non-uniform heating

2.1. *Problem formulation*

In the framework of the theoretical model developed in Part 1, onset of average convective motion is impossible without external heating. However, if homogeneity (or weak non-homogeneity, i.e. $\theta \ll \epsilon^2$) of the thermal boundary conditions is assumed, some terms that were neglected earlier should be taken into account. We begin from

the same basic equations as in Part 1:

$$\rho\left(\frac{\partial \boldsymbol{v}}{\partial t}+(\boldsymbol{v}\cdot\nabla)\boldsymbol{v}\right)=-\nabla p+\eta\Delta\boldsymbol{v}+\rho\boldsymbol{g}, \tag{2.1a}$$

$$\rho T\left(\frac{\partial S}{\partial t}+(\boldsymbol{v}\cdot\nabla)S\right)=\kappa\Delta T, \quad \frac{\partial\rho}{\partial t}+\nabla\cdot(\rho\boldsymbol{v})=0; \tag{2.1b}$$

$$p=p(\rho,T), \quad S=S(\rho,T). \tag{2.1c}$$

Here the same conventional notation is used. Following a derivation similar to that given in Part 1, the equations and boundary conditions describing weaker average effects are obtained:

$$\frac{\partial \boldsymbol{u}}{\partial t}+(\boldsymbol{u}\cdot\nabla)\,\boldsymbol{u}=-\nabla\Pi+\nu\Delta\boldsymbol{u}+g\beta T\boldsymbol{\gamma}, \quad \nabla\cdot\boldsymbol{u}=0, \tag{2.2a}$$

$$\frac{\partial T}{\partial t}+(\boldsymbol{u}\cdot\nabla)\,T+\frac{g}{a_T^2\beta}(\boldsymbol{u}\cdot\boldsymbol{\gamma})=\chi\Delta T+\frac{\partial}{\partial t}\langle T\rangle. \tag{2.2b}$$

Here $\boldsymbol{u}$, T are the velocity and temperature averaged over the period of vibration; t is the slow convective time; a_T^2, β, ν, χ are, respectively, the square of the isothermal sound speed, the thermal expansion coefficient, the viscosity and the thermal diffusivity coefficients, Π is the modified pressure, $\langle T\rangle$ is the temperature averaged over the container, $\boldsymbol{\gamma}$ is the unit vector along the z-axis (along gravity), and g is the intensity of gravity.

Since equations (2.2) do not contain the pulsating variables, we do not need to formulate the problem for the pulsation flow. The presence of vibrations becomes apparent in the additional generation of average temperature inhomogeneities, which is reflected in the effective boundary conditions:

$$\boldsymbol{u}=0, \quad T=T_B-\frac{\omega^2}{4a_T^4\beta}\Phi^2. \tag{2.3}$$

Here $\Phi=(\boldsymbol{j}\cdot\boldsymbol{r})$, where $\boldsymbol{j}$ is the unit vector along the axis of vibration, and $\boldsymbol{r}$ is the radius vector. The reference point for the potential Φ was discussed in Part 1. In equations (2.2) the state equation, $\rho=\rho_0-\rho_c\beta T-(\rho_c g/a_T^2)(\boldsymbol{\gamma}\cdot\boldsymbol{r})$, is used, i.e. the density non-homogeneities caused by temperature variations are comparable with the hydrostatic effect. The conservation of the whole fluid mass is also assumed.

If the boundary is not perfectly heat conducting (see §4.1 in Part 1), then the temperature boundary condition (second equation in (2.3)) needs to be rescaled by $(1+b)^{-2}$ (here $b=(\kappa/\kappa_B)\sqrt{\chi_B/\chi}$, where κ, χ, κ_B, χ_B are the heat conductivities and heat diffusivities of the fluid and wall, respectively).

To obtain dimensionless equations, L, L^2/χ, χ/L and θ (the imposed heating) are used as scales of length, time, velocity and temperature. In the dimensionless form, problem (2.2) becomes

$$\frac{1}{Pr}\left[\frac{\partial \boldsymbol{u}}{\partial t}+(\boldsymbol{u}\cdot\nabla)\,\boldsymbol{u}\right]=-\nabla\Pi+\Delta\boldsymbol{u}+Ra T\boldsymbol{\gamma}, \quad \nabla\cdot\boldsymbol{u}=0, \tag{2.4a}$$

$$\frac{\partial T}{\partial t}+(\boldsymbol{u}\cdot\nabla)T+\theta_g(\boldsymbol{u}\boldsymbol{\gamma})=\Delta T+\frac{\partial}{\partial t}\langle T\rangle. \tag{2.4b}$$

The effective boundary conditions in the dimensionless form are

$$\boldsymbol{u}=0, \quad T=T_B-\theta_w\Phi^2. \tag{2.5}$$

Here we have introduced new dimensionless parameters which characterize the ratios of imposed temperature difference to two internal generation sources of temperature non-homogeneities:

$$\theta_g = \frac{gL}{a_T^2}\frac{1}{\beta\theta}, \quad \theta_w = \frac{1}{4}\left(\frac{a\omega}{a_T}\right)^2\left(\frac{\omega L}{a_T}\right)^2\frac{1}{\beta\theta}. \tag{2.6}$$

2.2. *Equilibrium stability of a plane horizontal fluid layer in the absence of vibration*

Let us apply equations (2.4) with boundary conditions (2.5) to consider the stability of a plane layer. The physical statement of the problem is the same as for a similar problem examined in Part 1 (a horizontal layer of unit length and with fixed temperatures at the boundaries, $+1/2$ at the bottom boundary and $-1/2$ at the top), except that now we do not apply a vibrational forcing.

Equilibrium corresponds to the heat conducting temperature distribution. The problem of stability of this state with respect to the plane-normal perturbations can be reduced to the classical Rayleigh–Bénard problem: the problem of the stability of a plane horizontal layer of an incompressible fluid (the perturbations are assumed symmetric, therefore $\partial\langle T\rangle/\partial t = 0$). The solution of this problem is known – the critical Rayleigh number $Ra'_* = 1708$, where

$$Ra' = \frac{gL^3}{\nu\chi}\left(\beta\theta - \frac{gL}{a_T^2}\right). \tag{2.7}$$

The effect of compressibility can be thought of as a redefinition of the typical temperature difference that defines the Rayleigh number, taking into account the hydrostatic compression of the layer. This criterion is a sum of the Rayleigh and Schwarzschild criteria, which is in agreement with the theoretical works of Gitterman & Steinberg (1970), Raspo *et al.* (1999) and Kogan, Murphy & Meyer (1999), as well as with experiments by Ashkenazi & Steinberg (1999).

2.3. *Convective flow under isothermal boundary conditions*

Let us consider the case of isothermal boundary conditions: $T_B = 0$. We rewrite equations (2.4) and boundary conditions (2.5) using the amplitude of the temperature perturbations generated at the boundaries as a typical temperature scale. We then obtain

$$\frac{1}{Pr}\left[\frac{\partial \boldsymbol{u}}{\partial t} + (\boldsymbol{u}\cdot\nabla)\,\boldsymbol{u}\right] = -\nabla\Pi + \Delta\boldsymbol{u} + Ra_w T\boldsymbol{\gamma}, \quad \nabla\cdot\boldsymbol{u} = 0, \tag{2.8a}$$

$$\frac{\partial T}{\partial t} + (\boldsymbol{u}\cdot\nabla)\,T + \theta_{gw}\,(\boldsymbol{u}\cdot\boldsymbol{\gamma}) = \Delta T + \frac{\partial}{\partial t}\langle T\rangle. \tag{2.8b}$$

The boundary conditions are

$$\boldsymbol{u} = 0, \quad T = -\Phi^2. \tag{2.9}$$

Here new parameters are introduced:

$$Ra_w = \frac{1}{4}\frac{(a\omega L)^2}{\nu\chi}\frac{(\omega L)^2}{a_T^2}\frac{gL}{a_T^2}, \qquad \theta_{gw} = 4\frac{a_T^2}{(a\omega)^2}\frac{a_T^2}{(\omega L)^2}\frac{gL}{a_T^2}. \tag{2.10}$$

Based on these equations and boundary conditions, the fluid behaviour inside a cylindrical container of circular cross-section subjected to translational vibration perpendicular to the cylinder axis was considered.

Quasi-equilibrium is impossible in this case. Let us consider the flow structrure at small values of θ_{gw} and Ra_w, applying the creeping flow approximation. Assume that

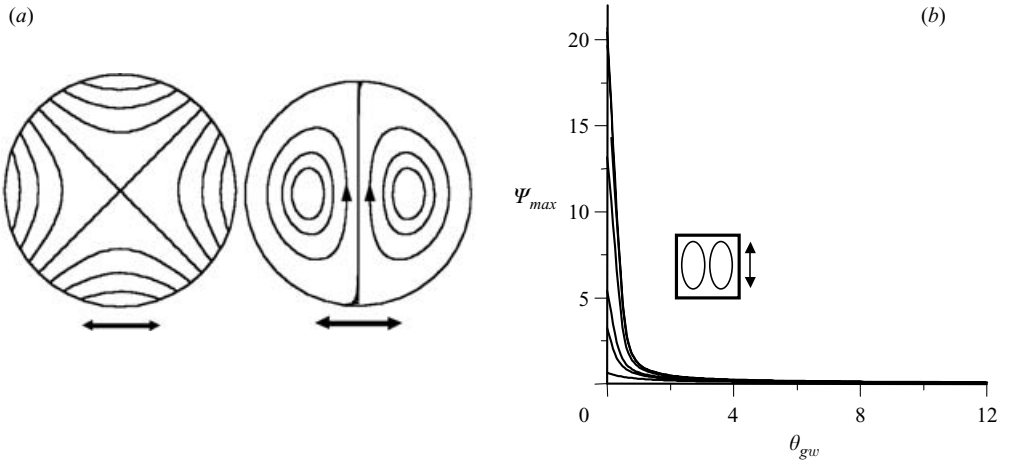

FIGURE 2. (*a*) Isotherms (left) and structure (right) of the average flow for horizontal vibrations. Isothermal boundary conditions, under gravity. (*b*) Average flow intensity vs. ratio of hydrostatic to vibrational temperature non-homogeneities at different values of the Rayleigh number ($Ra_w = 10^4$ to 10^6) for a square cavity. For $Ra_w = 10^6$ the curves for several Prandtl numbers (in the range of 1–20) are obtained, which almost coincide.

the axis of vibraition is inclined at an angle α to the horizontal x-axis. The field Φ, in this case, may be represented in the form

$$\Phi = r\cos(\phi - \alpha), \tag{2.11}$$

where r is the polar radius and ϕ is the azimuthal angle measured from the horizontal axis. The steady-state temperature field in the leading approximation may be derived by solving the Laplace equation with boundary conditions (2.9) at $r = 1$, and the solution is

$$T = -\tfrac{1}{2}(1 + r^2\cos(2(\phi - \alpha))). \tag{2.12}$$

Then, we introduce the stream function ψ for the average flow through the relation, $\boldsymbol{u} = \nabla\psi \times \boldsymbol{k}$, where $\boldsymbol{k}$ is the unit vector along the cylinder axis. By using (2.8) and omitting the nonlinear and non-stationary terms, we obtain the following equation defining ψ:

$$\Delta\psi = Ra_w \boldsymbol{k} \cdot (\nabla T \times \boldsymbol{\gamma}). \tag{2.13}$$

The solution of this equation, that satisfies the no-slip boundary condition at $r = 1$, is

$$\psi = -\frac{Ra_w}{192} r(1 - r^2)^2 \cos(\phi - 2\alpha). \tag{2.14}$$

This solution determines flow with a two-vortex structure for any value of angle α. The plane separating the vortices is given by

$$\phi_* = \frac{\pi}{2} + 2\alpha. \tag{2.15}$$

Thus, the boundary plane between the vortices is vertical in cases of both vertical and horizontal vibrations. However, the flow directions are opposite: the flow in the centre of a cavity moves upwards under vertical vibrations (figure 2*a*), and downwards under horizontal ones. If the axis of vibration is inclined to the horizontal axis at the angle $\alpha = \pi/4$, the plane separating the vortices is horizontal.

In a cylinder of square cross-section, the flow structure at small θ_{gw} and Ra_w is qualitatively the same as in the case of a circular cylinder. Numerical calculations performed for finite values of parameters θ_{gw} and Ra_w show that the quasi-equilibrium state is also impossible. The average flow has a two-vortex pattern. The growth of the Rayleigh number leads to intensification of flow, whereas increase of the gravity stratification (parameter θ_{gw}) leads to the reverse effect: the flow intensity strongly decreases (figure 2*b*).

3. Isothermal cavity under weightlessness

The most interesting result obtained in the preceding § 2 is a possibility of inducing the average temperature variations by vibration, which was shown to result in convective flows even in an isothermal container. Here we examine problems where the average motion is induced by this near-critical mechanism in zero gravity conditions. Another aim of the section is to compare the results obtained using the system of averaged equations with the results by Jounet *et al.* (2000) obtained by direct numerical simulations using the Navier–Stokes equations for a compressible medium.

We consider an isothermal container filled with a near-critical fluid under microgravity conditions. The container undergoes translational vibrations with linear polarization. The pulsation velocity (the leading term of the pulstational velocity of the fluid equals the velocity of the container, see Part 1) may be represented as $\boldsymbol{w}_0 = a\omega \boldsymbol{j}\cos(\omega t)$, where $\boldsymbol{j}$ is a unit vector of the axis of vibration; the potential of the pulsation velocity is $\Phi = a\omega L(\boldsymbol{j}\cdot\boldsymbol{r})$, where $\boldsymbol{r}$ is a non-dimensional radius vector.

The average flow cannot be described with the equations given above: the finer effects have to be taken into account. To obtain the governing equations we start with (2.1) and consider small temperature non-homogeneities induced solely by vibrations. The Boussinesq parameter is chosen as a small parameter of the problem $\beta\theta_w = \epsilon \ll 1$. Applying the standard averaging procedure (the derivation is almost identical to the derivation of equations and boundary conditions given in Part 1: the initial equations are the same, only the small parameter is defined differently, but this does not affect the course of the derivation), one obtains the equations for average and pulsating fields:

$$\frac{\partial \boldsymbol{u}}{\partial t} + (\boldsymbol{u}\cdot\nabla)\,\boldsymbol{u} = -\nabla\Pi + \nu\Delta\boldsymbol{u} + 2\overline{(\boldsymbol{w}\cdot\boldsymbol{w}_0)}\beta\nabla T + (\sigma-1)\left(\frac{\omega}{c}\right)^2\overline{\Phi^2}\beta\nabla T, \quad (3.1a)$$

$$\frac{\partial T}{\partial t} + (\boldsymbol{u}\cdot\nabla)T = \chi\Delta T + \frac{\partial}{\partial t}\langle T\rangle, \quad \langle T\rangle = \frac{1}{V}\int_V T\,\mathrm{d}V, \quad (3.1b)$$

$$\nabla\cdot\boldsymbol{u} = 0; \quad (3.1c)$$

$$\beta\tilde{T} = -\frac{a}{L}\left(\frac{\omega L}{c}\right)^2\gamma\,(\boldsymbol{j}\cdot\boldsymbol{r})\sin\omega t, \quad (3.2)$$

$$\nabla\times\boldsymbol{w} = \beta\nabla T\times\boldsymbol{w}_0, \quad \nabla\cdot\boldsymbol{w} = -\left(\frac{\omega}{c}\right)^2\Phi. \quad (3.3)$$

Here $\overline{(\ldots)}$ denotes time-averaging. The effective boundary conditions are

$$T = -\frac{a^2\omega^4L^2}{4a_T^2\beta a_T^2}(\boldsymbol{j}\cdot\boldsymbol{r})^2, \quad \boldsymbol{u} = 0; \quad (3.4a)$$

$$w_n = a\omega\left(\frac{\omega L}{c}\right)^2\gamma\frac{\delta_\chi}{L}(\boldsymbol{j}\cdot\boldsymbol{r})(\cos(\omega t)+\sin(\omega t)). \quad (3.4b)$$

These equations describe convective flows, which could be generated only in a near-critical fluid (owing to its particular properties). In Part 1, in the resulting effective boundary condition for pulsation flows, the term proportional to $\sin(\omega t)$ was omitted since we focused there on average effects unaffected by this addition. Now the structure of the pulsation flows is equally important, so we keep this term.

We apply the system (3.1)–(3.4) to consider flows in an isothermal plane layer and isothermal cylindrical cavities of square cross-section (following Jounet *et al.* 2000) and circular cross-section. The model of a near-critical fluid adopted in the works of Carles & Zappoli (1995) and Jounet *et al.* (2000) is used, namely: the van der Waals state equation, constancy of viscosity coefficient, isochoric heat capacity and isentropic sound speed, together with the following law for the heat conductivity: $\kappa = \kappa_0(1 + \kappa_1 t^{-0.5})$, where $\kappa_0 = 10^{-2}\,\mathrm{W\,(m\,K)^{-1}}$, $\kappa_1 = 0.75$, $t = (T - T_c)/T_c$ (values of κ_0, κ_1 are taken for CO_2). Critical parameters for carbon dioxide CO_2 ($T_c = 304.1\,\mathrm{K}$, $\rho_c = 467.8\,\mathrm{kg\,m^{-3}}$, $p_c = 7.378\,\mathrm{M\,Pa}$, dynamic viscosity: $\eta_0 = 3.45 \times 10^{-5}\,\mathrm{kg\,(m\,s)^{-1}}$) are applied.

3.1. *One-dimensional results*

Let us consider a plane layer of a near-critical fluid and subjected to transversal vibrations. Both boundaries of the layer are maintained at the same temperature.

The problem allows a solution that corresponds to the quasi-equilibrium state. In this state the average temperature field in a layer is homogeneous and equals $T = -a^2\omega^4 L^2/(16 a_T^4 \beta)$, where L is the layer thickness.

Equations (3.3) give the following quasi-equilibrium distribution of the pulsating velocity in a layer:

$$w_x = 0, \quad w_z = \tfrac{1}{2} a\omega \left(\frac{\omega L}{c}\right)^2 \left[\left(\tfrac{1}{4} - z^2\right)\cos(\omega t) + \gamma \frac{\delta_\chi}{L}(\cos(\omega t) + \sin(\omega t))\right], \qquad (3.5)$$

where z is the dimesionless transversal coordinate in units of L and with origin in the middle of the layer. The profile coincides with the results of Carles & Zappoli (1995).

Let us estimate the typical orders of different physical values, restricting ourselves to the following cases:

(a) $\Delta T = 15\,\mathrm{mK}$, $A = 0.1\,\mathrm{m\,s^{-2}}$, $f = 5\,\mathrm{Hz}$;
(b) $\Delta T = 0.1\,\mathrm{K}$, $A = 10\,\mathrm{m\,s^{-2}}$, $f = 3\,\mathrm{k\,Hz}$;
(c) $\Delta T = 0.2\,\mathrm{K}$, $A = 0.1\,\mathrm{m\,s^{-2}}$, $f = 20\,\mathrm{Hz}$.

The thickness of the layer is $L = 1\,\mathrm{cm}$. Here $A = a\omega^2$ is the amplitude of vibrational acceleration and $f = \omega/2\pi$.

The typical values of the pulsation temperature non-homogeneities (according to (3.2)) are: (a) $|\tilde{T}| = 1.77 \times 10^{-6}\,\mathrm{K}$, ($b$) $|\tilde{T}| = 1.77 \times 10^{-4}\,\mathrm{K}$, ($c$) $|\tilde{T}| = 1.77 \times 10^{-6}\,\mathrm{K}$. The amplitude of the pulsation temperature does not depend on the proximity to the critical point and is determined by the amplitude and frequency of the vibrational forcing only.

The values of the average temperature non-homogeneities are: (a) $|T| = 3.48 \times 10^{-11}\,\mathrm{K}$, ($b$) $|T| = 5.20 \times 10^{-9}\,\mathrm{K}$, ($c$) $|T| = 2.60 \times 10^{-12}\,\mathrm{K}$.

3.2. *Square cavity*

The problem considered by Jounet *et al.* (2000), which is the main source for the present comparison, is characterized by the absence of gravity and external temperature differences. The only reason for fluid motion is diverging compressibility of a near-critical medium. Perceptible pulsation and especially average flows are

	Pr	Ra_v	Ra_a	Ra_{PE}
(a)	72.7	4.33×10^{-10}	1.34×10^{-7}	2.39×10^{-7}
(b)	46.8	6.08×10^{-7}	3.02	7.52×10^{-2}
(c)	32.8	2.29×10^{-17}	2.02×10^{-10}	3.68×10^{-10}

TABLE 1. Values of dimensionless parameters corresponding to real situations.

generated only by sufficiently strong vibrations. Equations and boundary conditions describing these average and pulsation fields in non-dimensional form are

$$\frac{1}{Pr}\left[\frac{\partial \boldsymbol{u}}{\partial t}+(\boldsymbol{u}\cdot\nabla)\,\boldsymbol{u}\right]=-\nabla\Pi+\Delta\boldsymbol{u}+2\left(\left(\boldsymbol{w}^{(1)}+\boldsymbol{w}^{(2)}\right)\cdot\boldsymbol{j}_0\right)\nabla T + \frac{\sigma-1}{2}Ra_a z^2\nabla T, \quad (3.6a)$$

$$\frac{\partial T}{\partial t}+(\boldsymbol{u}\cdot\nabla)\,T=\Delta T+\frac{\partial}{\partial t}\langle T\rangle, \quad (3.6b)$$

$$\nabla\cdot\boldsymbol{u}=0; \quad (3.6c)$$

$$\nabla\times\boldsymbol{w}^{(1)}=Ra_v\,(\nabla T\times\boldsymbol{j})\cos(\omega t),\quad \nabla\cdot\boldsymbol{w}^{(1)}=0; \quad (3.7a)$$

$$\nabla\times\boldsymbol{w}^{(2)}=0,\quad \nabla\cdot\boldsymbol{w}^{(2)}=-Ra_a z\cos(\omega t); \quad (3.7b)$$

$$w_n^{(1)}=0,\quad w_n^{(2)}=Ra_{PE}z\,(\cos(\omega t)+\sin(\omega t)). \quad (3.7c)$$

Here L, L^2/χ, χ/L, θ, $a\omega$, $a\omega L$ are used as units of length, time, average velocity, temperature, pulsation velocity $\boldsymbol{w}_0$ and potential Φ. The quantity $\boldsymbol{w}$ is represented as the sum of two components with the scale $2\nu\chi/(a\omega\beta\theta L^2)$.

Boundary conditions for the average fields are

$$T=-z^2,\quad \boldsymbol{u}=0. \quad (3.8)$$

The following non-dimensional parameters are introduced:

$$Pr=\frac{\nu}{\chi},\quad \beta\theta=\frac{a^2\omega^4L^2}{4a_T^4},\quad Ra_v=\frac{1}{2}\frac{(a\omega L)^2}{\nu\chi}(\beta\theta)^2, \quad (3.9a)$$

$$Ra_a=\frac{1}{2}\frac{(a\omega L)^2}{\nu\chi}\beta\theta\left(\frac{\omega L}{c}\right)^2,\quad Ra_{PE}=\frac{1}{2}\frac{(a\omega L)^2}{\nu\chi}\beta\theta\left(\frac{\omega L}{c}\right)^2\gamma\frac{\delta_\chi}{L}. \quad (3.9b)$$

Estimations of these values for the cases enumerated above are given in table 1. As one can see, the generation of perceptible average flows is possible only for case (b) when the vibrations are sufficiently strong. Of course, if gravity or external temperature gradients are added, the average flows become non-negligible as is also the case for moderate vibrations. The typical values of the temperature non-homogeneities (both pulsation and average) would be the same as for a plane layer.

Jounet *et al.* (2000) obtained the square cavity for the pulsation fields for parameters corresponding to case (c). These fields are used for the present comparison.

The results obtained by the finite-difference method are given in figures 3. The simple asymptotic equations (3.7a) give precisely the same field structures as reported in the work of Jounet *et al.* (2000), which were obtained through difficult numerical computations. Moreover, we are able to consider the average fields (case b). The averaging approach also allows the flows in more sophisticated configurations to be examined, whereas by direct numerical simulations, even a cavity of circular cross-section could not be treated.

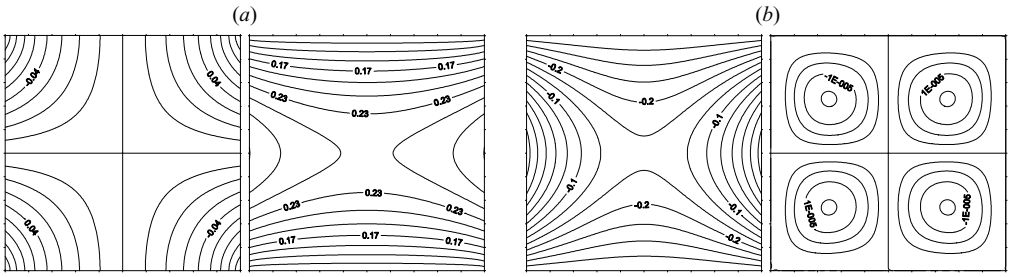

FIGURE 3. (*a*) x- (left) and z- (right) components of the pulsation velocity for $\omega t = 0$. Vibrations are imposed along the vertical z-axis. $\Delta T = 0.2\,\mathrm{K}$, $A = 0.1\,\mathrm{m\,s^{-2}}$, $f = 20\,\mathrm{Hz}$. (*b*) Average temperature (left) and velocity fields (right). $\Delta T = 0.1\,\mathrm{K}$, $A = 10\,\mathrm{m\,s^{-2}}$, $f = 3\,\mathrm{k\,Hz}$.

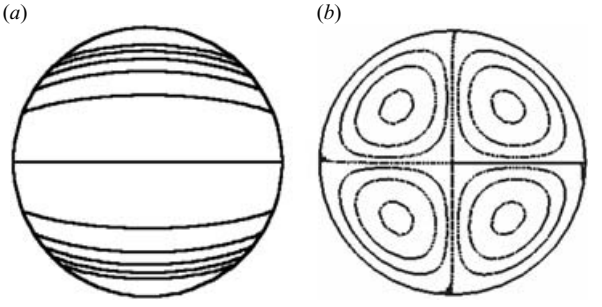

FIGURE 4. (*a*) Structure of the pulsation field for const = 0, 0.25, 0.75, 1.25, 1.75, 2.25, $\gamma/\delta_\chi L = 0.2$, $\omega t = 0$. (*b*) Structure of average flow for $\sigma = 3$, $Ra_a = 1$. Isothermal boundary, weightlessness.

3.3. *Circular cavity*

Let us consider the influence of translational vibrations on a cylindrical cavity of circular cross-section filled with a near-critical fluid. The cavity walls are maintained at a fixed temperature. Gravity is not imposed.

The pulsation temperature field generated by such vibrations is

$$\beta\tilde{T} = -\frac{a}{L}\left(\frac{\omega L}{c}\right)^2 \gamma x \sin(\omega t). \tag{3.10}$$

The pulsation velocity field is determined by the following equations and boundary conditions (vibrations are directed along the x-axis):

$$\nabla \times \boldsymbol{w} = 0, \quad \nabla \cdot \boldsymbol{w} = -a\omega\left(\frac{\omega L}{c}\right)^2 x\cos(\omega t), \tag{3.11a}$$

$$r = 1: \quad w_r = a\omega\left(\frac{\omega L}{c}\right)^2 \gamma\frac{\delta_\chi}{L}x(\cos(\omega t) + \sin(\omega t)). \tag{3.11b}$$

We cannot introduce the stream function to characterize the pulsation flow since this field is non-solenoidal. Nevertheless, it is still possible to represent the flows with integral curves of the velocity field, by integrating the following expression:

$$\frac{\mathrm{d}r}{\mathrm{d}\phi} = r\frac{w_r}{w_\phi}. \tag{3.12}$$

These lines are plotted in figure 4 for several constants of integration, const.

Further, the average hydrodynamic fields, defined by

$$\frac{1}{Pr}\left[\frac{\partial \boldsymbol{u}}{\partial t}+(\boldsymbol{u}\cdot\nabla)\,\boldsymbol{u}\right]=-\nabla\Pi+\Delta\boldsymbol{u}+Ra_a A\nabla T, \tag{3.13a}$$

$$\frac{\partial T}{\partial t}+(\boldsymbol{u}\cdot\nabla)\,T=\Delta T+\frac{\partial}{\partial t}\langle T\rangle, \quad \nabla\cdot\boldsymbol{u}=0; \tag{3.13b}$$

$$A=-\frac{r^2}{8}(1+2\cos^2\phi)+\frac{\sigma-1}{2}r^2\cos^2\phi, \tag{3.13c}$$

$$r=1: \quad \boldsymbol{u}=0, \quad T=-\cos^2\phi, \tag{3.13d}$$

are analysed. Only the stationary solution within the creeping-flow approximation ($Ra_a\to 0$) is examined.

Derivations similar to those described in § 2.3 give the following results:

$$T=-\frac{1}{2}(1+r^2\cos 2\phi), \quad \psi=\frac{Ra_a\sigma}{768}r^2(1-r^2)^2\sin 2\phi. \tag{3.14}$$

The temperature profile is the same as for the isothermal cavity under terrestrial gravity considered in § 2.3 and plotted in figure 2(*a*). The structure of the average flow is shown in figure 4(*b*). This flow consists of four vortices while, under a gravity field, an isothermal flow is composed of two vortices (figure 2*a*).

The structures of the flows obtained both for zero gravity and terrestrial conditions are close to the experimental results (see Beysens & Garrabos 2001; Zyuzgin *et al.* 2001) on thermal vibrational convection obtained in the framework of the 'ALICE' (Analyse des Liquides Critiques dans l'Espace) project. Here, a convective slot was filled with a near-critical fluid. A heater was placed in the centre and set the temperature of the fluid. The slot was subjected to transversal vibrations. Under high-frequency vibrations, average flows were observed with a four-vortex structure in weightlessness and with two vortices in terrestrial conditions, i.e. the same as in figures 2(*a*) and 4(*b*).

4. Classification of the models

In this section we discuss why, when describing the thermal vibrational convection in a near-critical fluid, we formulate three different theoretical models described in Part 1 and here.

The difference in the proposed theoretical models is mainly related to the order of temperature variations. The non-dimensional temperature variations are defined by $\theta=\theta'/T_c$ (θ' is a dimensional quantity). First, as was mentioned at the beginning, we do not consider the case $\theta\sim(T_0-T_c)/T_c=\epsilon$ since in this case we could not guarantee that the fluid remained single phase.

The case considered in Part 1 is called 'non-uniform heating'. That means there is external heating (or cooling) with typical amplitude $\theta=\epsilon^2$. The theoretical model formulated differs from the model used for incompressible fluids (Gershuni & Lyubimov 1998): several new effects are introduced by additional parameters, mainly responsible for the diverging compressibility of a near-critical medium. The intensity of flows is governed by the thermal Rayleigh number Ra and three analogues of these numbers: Ra_v, Ra_a, and Ra_{PE}.

Here, in Part 2, we deal with the case of 'weakly non-uniform heating' which means the external heating is of the order $\theta\ll\epsilon^2$. Against the background of such small temperature variations, we have to take into account the hydrostatic effect and the

average temperature variations induced by vibrations. The relations between these quantities and the external temperature difference are characterized by the parameters θ_g and θ_w (2.6). The intensity of convective motion is defined just by the thermal Rayleigh number Ra and the effects governed by the vibrational analogues of the Rayleigh number have been proved negligible. Indeed, if one assumes that $\theta_w, \theta_g \sim 1$, then e.g. $Ra/Ra_a = \frac{1}{2}(\theta_g/\theta_w)\gamma \to \infty$, since $\gamma = c_p/c_V \to \infty$. Hence, buoyancy-driven flows predominate. Since there are three sources of temperature non-homogeneities, we may make one of them (e.g. external gradients) tend to zero. That gives us the problem for convective flows under isothermal boundary conditions.

The third theoretical model is formulated in § 3 of this paper. We assume weightlessness and the absence of the external temperature differences. In this case only weak flows of vibrational origin remain. These flows may be significant only under rather intensive vibrational influence (with a frequency of the order of several k Hz).

5. Discussion and conclusions

In Part 1 and here we have examined the influence of vibration and gravity on the behaviour of a single-phase near-critical fluid. The main results are two closed theoretical models of thermal vibrational convection for two different types of imposed heating, and a model for one exceptional case of isothermal boundaries and weightless conditions. Anomalously high compressibility and heat conductivity of a fluid result in qualitative differences of the equations from the standard theory (Gershuni & Lyubimov 1998).

In the derivation of the equations of Part 1, we assumed that non-homogeneities of average density appeared in the leading order of expansion. Here we focused on the effects of vibration and gravity stratifications: we supposed that the average density was homogeneous at leading order and could vary only at the next orders. The imposed temperature non-homogeneities are necessarily small in this case (weakly non-uniform heating). Nevertheless, as was shown, the generation of convective motion remains possible in a near-critical fluid even in the complete absence of external heating.

The equations obtained here in § 2 are mainly the same as the equations of thermal vibrational convection, which take compressibility into account in the acoustical sense (see Lyubimov 2000). The main difference becomes apparent in the equation of state. Because of anomalously high mechanical compressibility, density variations are caused not only by temperature variations, but also by the changes in average pressure. These changes are determined by two additional factors: average pressure, related to pulsation velocity field, and hydrostatic stratification.

The sharp distinctions between the present work and the classical theory are in the new non-trivial boundary condition for the average temperature field (2.3). This results in a fundamentally new mechanism for the generation of the average flow. Usually vibrations can generate the average flow through the vibrational force or through the Schlichting boundary condition. Neither of these mechanisms is at work but, nevertheless, vibrations are still able to induce non-homogeneities in temperature, which result in the onset of the usual convective flows under gravity.

In particular, these assumptions explain the difference in the results for stability of a plane horizontal fluid layer. In Part 1 the temperature gradient, caused by gravity stratification, was assumed to be small in comparison with external heating of a layer. That is why the Schwarzschild criterion was unimportant and was not taken into consideration. Here, the Schwarzschild criterion is essential (2.7).

To derive the governing equations determining the flows in an isothermal cavity under weightlessness (§ 3), a somewhat different approach was applied. The scale of non-homogeneities in the temperature field here is associated only with vibrational forcing. On the basis of this scale we formed the Boussinesq parameter. Assuming the smallness of this parameter we obtain the equations of vibrational convection.

For this last case we had the possibility to verify the equations obtained by comparison with previously performed direct numerical simulations (Jounet *et al.* 2000). Unfortunately, only pulsation flows had been considered by the direct approach, since the average flows are noticeable only under intense vibrational influence, unattainable in direct calculations. Nevertheless, the pulsational fields coincide quite well. We were also able to predict the structures of the average fields, which proved to be similar to the recent experimental results reported by Beysens & Garrabos (2001) and Zyuzgin *et al.* (2001).

This work was supported by (i) Award No. PE-009-0 from the U.S. Civilian Research & Development Foundation for the Independent States of the Former Soviet Union (CRDF); (ii) grant from the Russian Foundation for Basic Research No. 0001-00450; (iii) programme of financial support for Leading Scientific Schools, grant No. 00-15-96112; (iv) and within the framework of Reseau formation-recherche franco-russe of MENRT-DRIC.

REFERENCES

Ashkenazi, Sh. & Steinberg, V. 1999 High Reyleigh number turbulent convection in a gas near the gas-liquid critical point. *Phys. Rev. Lett.* **83**, 3641–3644.

Beysens, D. & Garrabos, Y. 2001 Near-critical fluids under microgravity: status of the ESEME program and perspectives for the ISS. *Acta Astraunatica* **48**, 629–638.

Carles, P. & Zappoli, B. 1995 The unexpected response of near-critical fluids to low-frequency vibrations. *Phys. Fluids* **7**, 2905–2914.

Gershuni, G. Z. & Lyubimov, D. V. 1998 *Thermal Vibrational Convection*. Wiley & Sons.

Gitterman, M. Sh. & Steinberg, V. A. 1970 Criteria for the commencement of convection in a liquid close to the critical point. *Teplofyz. Vys. Temp. [High Temp. (USSR)]* **8**, N 4, 799–805, in Russian.

Jounet, A., Mojtabi, A., Ouazzani, J. & Zappoli, B. 2000 Low-frequency vibrations in a near-critical fluid. *Phys. Fluids* **12**, 197–204.

Kogan, A. B., Murphy, D. & Meyer, H. 1999 Rayleigh-Benard convection onset in a compressible fluid: 3He near Tc. *Phys. Rev. Lett.* **82**, 4635–4638.

Lyubimov, D. V. 2000 Thermal convection in an acoustic field. *Fluid Dyn.* **35**, 321–330.

Lyubimov, D., Lyubimova, T., Vorobev, A., Mojtabi, A. & Zappoli, B. 2006 Thermal vibrational convection in near critical fluids. Part 1. Non-uniform heating. *J. Fluid Mech.* **564**, 159–183.

Raspo, I., Gilly, B., Amiroudine, S., Bontoux, P. & Zappoli, B. 1999 Simulation of convective instabilities inside a supercritical fluid layer under Rayleigh-Benard configuration. *J. Chim. Phys.* **96**, 1059–1065.

Zyuzgin, A. V., Ivanov, A. I., Polezhaev, V. I., Putin, G. F. & Soboleva, E. B. 2001 Convective motions in near-critical fluids under real zero-gravity conditions. *Cosmic Res.* **39**, 175–186.